Analytic Solution for Optimal Two-Impulse 180° Transfer between Noncoplanar Orbits and the Optimal Orientation of the Transfer Plane

FANG TOH SUN*
NASA Electronic Research Center, Cambridge, Mass.

An analytic solution in closed form for the optimal two-impulse transfer through a range angle of 180° with minimum total velocity impulse is presented. The solution is valid for the transfer between two noncoplanar Keplerian orbits under arbitrary terminal conditions, in a transfer plane of any arbitrary orientation. The total impulse is further minimized by optimizing the orientation of the transfer plane. A brief treatment of the coplanar case is included following the general solution. Numerical solutions under some typical terminal conditions are also presented, and several modes of transfer compared. In the light of the analytic solution and the numerical results, the effects of terminal conditions on the optimal two-impulse transfer are discussed.

Nomenclature

A	= distance between the terminal velocity constraining line and the radial axis
$\mathbf{e}$	= unit vector
f	= total velocity impulse
f_i	= terminal velocity impulse ($i = 1,2$)
h	= angular momentum vector (per unit orbiting mass)
n	= r_2/r_1
$\mathbf{r}$	= position vector
$\mathbf{v}$	= velocity
$\Delta\mathbf{v}_i$	= terminal velocity increment = $\mathbf{v}_i - \mathbf{v}_{0i}$ ($i = 1,2$)
γ	= direction angle relative to the local radial direction
Λ	= inclination of the velocity-increment plane to the transfer plane
μ	= strength of the Newtonian gravity field
ρ_i	= terminal parameter, defined by Eqs. (15), ($i = 1,2$)
ν	= local circular speed ratio = $v/(\mu/r)^{1/2}$
σ	= dihedral angle between the terminal orbit planes
ω	= inclination of the terminal orbit plane to the transfer plane

Subscripts

0	= terminal condition, initial or final
1,2	= terminal point
h	= component normal to the the plane of motion
J	= pertaining to the joint type optimal orientation curve
r	= radial component
θ	= transversal component in the transfer plane
Θ	= transversal component in the terminal orbit plane
$(\ )_*$	= foot of perpendicular to the velocity constraining line
$(\ )_{**}$	= two-impulse optimum
Δ	= pertaining to velocity increment

Superscripts

$(\ )^*$	= critical (parabolic)

I. Introduction

THE two-impulse orbital transfer through a range angle of 180° with minimum total velocity impulse is of both theoretical and practical importance as it is usually the simplest mode of economic transfer. However, no analytic solution is available so far, except in some highly restricted cases, such as the coplanar transfer via Hohmann ellipse,[1] or the transfer in the near vicinity of a circular orbit.[10] Furthermore, when the two terminal orbits are noncoplanar, the 180° transfer permits the choice of the transfer plane, since the two terminal position vectors, being collinear, do not determine the orientation of the transfer plane, and leaves an additional degree of freedom at our disposal. Such a feature is not found in non-180° transfers.

In the following, an analytic solution in closed form will be first presented for the noncoplanar transfer in an arbitrary transfer plane. The two terminal orbits are assumed to be Keplerian, with no restrictions on their eccentricities and orientations, nor any restrictions on the terminal distances and the initial and final orbital velocities. It is to be noted that the general equation governing the two-impulse optimum for an arbitrary non-180° range angle, known as the optimum octic,[6,7,12] does not apply in the present case. It is easy to see that Altman and Lee's equations[6,7] both reduce to identities in the 180° transfer, and in Sun's equation in the oblique velocity coordinates[12] the real roots tend to infinity as the range angle approaches π. In the following treatment, instead of reformulating with some new variables, a geometric approach in the velocity-space will be employed, and the optimum law of equal slope[12] will be applied. It will be seen that such an approach leads directly to the analytic solution required, which is valid for any arbitrary transfer plane containing the two terminal position vectors. The total velocity impulse thus obtained will then be further minimized by optimizing the orientation of the transfer plane for a fixed oblique angle between the two terminal planes.

II. Optimal Transfer in an Arbitrary Transfer Plane

Let the orientation of the transfer plane and those of the terminal orbit planes each be specified by a unit normal vector in the direction of the angular momentum vector of the transfer trajectory or the orbit in the plane,

$$\mathbf{e}_h = \mathbf{h}/h,\ \mathbf{e}_{h1} = \mathbf{h}_1/h_1,\ \mathbf{e}_{h2} = \mathbf{h}_2/h_2 \tag{1}$$

and denote the dihedral angle between the terminal orbit planes by σ, and their inclinations with the transfer plane by ω_1 and ω_2, so that

$$\cos\sigma = \mathbf{e}_{h1}\cdot\mathbf{e}_{h2},\ \cos\omega_1 = \mathbf{e}_{h1}\cdot\mathbf{e}_h,\ \cos\omega_2 = \mathbf{e}_{h2}\cdot\mathbf{e}_h \tag{2}$$

Presented as Paper 68-093 at the AAS/AIAA Aerodynamics Specialist Conference, Jackson, Wyo., September 3–5, 1968; submitted December 4, 1968; revision received May 29, 1969. This work was done at the Wichita State University under NASA Grant NGR 17-003-008.

* Senior Research Associates, NAS-NRC. Member AIAA.

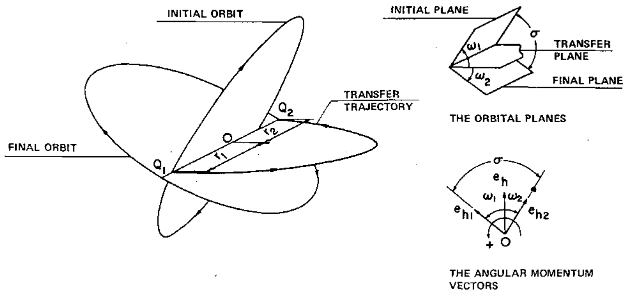

Fig. 1 Geometry of 180° transfer between noncoplanar orbits.

For convenience, we restrict the angles to be

$$0 \leqslant \sigma \leqslant \pi, \quad -\pi \leqslant \omega_1 \leqslant \pi, \quad -\pi \leqslant \omega_2 \leqslant \pi$$

where the positive direction for the angular measurement is chosen to be from $\mathbf{e}_{h1}$ to $\mathbf{e}_{h2}$. Clearly, no generality is lost by such restrictions, and we have

$$\sigma = \omega_1 - \omega_2 \tag{3}$$

in all cases.

The transfer geometry in the position-space, and that in the velocity-space are shown in Figs. 1 and 2. The problem is to minimize the quantity

$$f = f_1 + f_2 \tag{4}$$

where

$$f_i = |\mathbf{V}_i - \mathbf{V}_{0i}| \; (i = 1,2) \tag{5}$$

when the terminal conditions specified by r_1, r_2, $\mathbf{V}_{01}$, $\mathbf{V}_{02}$, and ω_1 and ω_2 are fixed. Before proceeding to the optimization, two peculiar characteristics of 180° transfer are to be noted. First, in a given Newtonian field, the scalar angular momentum of the transfer trajectory is determined by the two terminal distances, r_1 and r_2 only, hence independent of the choice of the particular trajectory, in accordance with[4,8]

$$h = [2\mu r_1 r_2/(r_1 + r_2)]^{1/2} \tag{6}$$

It follows that, for two fixed terminal points, the transversal component of the transfer velocity at each terminal is a constant, given by

$$A_1 = \left(\frac{2\mu r_2/r_1}{r_1 + r_2}\right)^{1/2}, \qquad A_2 = \left(\frac{2\mu r_1/r_2}{r_1 + r_2}\right)^{1/2} \tag{7}$$

This fact is manifested in the velocity-space by the two constraining lines in the transfer plane, parallel to the radial axis, one for each terminal, on which the tip of the transfer velocity at that terminal is to be confined[12] (Fig. 2). Their distances from the radial axis are given by Eqs. (7). Second, the two radial components of the terminal transfer velocities are equal,[4] i.e.,

$$\mathbf{V}_{r1} = \mathbf{V}_{r2} \tag{8}$$

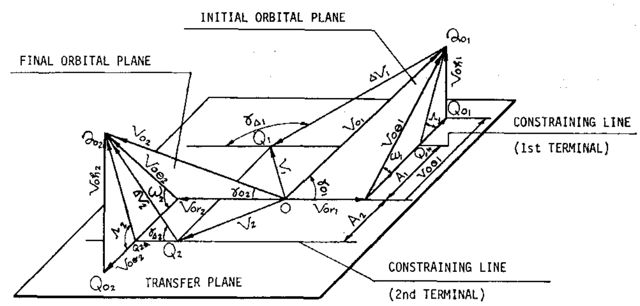

Fig. 2 Geometry of velocity vectors for 2-impulse 180° transfer.

As shown in Fig. 2, $\mathcal{Q}_{01}$ and $\mathcal{Q}_{02}$ are the tips of the two terminal orbit velocity vectors, and Q_1 and Q_2 are an arbitrary pair of transfer points located on the respective constraining lines. The line connecting Q_1 and Q_2 is then necessarily perpendicular to both constraining lines in view of Eq. (8). Now by translating these two constraining lines with the corresponding velocity-increment vectors rigidly attached to each, until the points Q_1 and Q_2 coincide, we obtain the first simplified hodograph diagram of Fig. 3a. The problem is then to minimize the total distance $|\overline{\mathcal{Q}_{01}Q_1}| + |\overline{\mathcal{Q}_{02}Q_2}|$ in the velocity-space. As shown in Ref. 12, the optimum condition is given by the equal-slope law, which, for the three-dimensional case, may be written

$$\sin\gamma_{\Delta 1} = \sin\gamma_{\Delta 2} \tag{9}$$

where $\gamma_{\Delta 1}$ and $\gamma_{\Delta 2}$ are the direction angles of $\Delta\mathbf{V}_1$ and $\Delta\mathbf{V}_2$ measured from the respective local radial directions. Thus by rotating the two velocity-increment planes, defined by $\mathbf{r}$ and $\Delta\mathbf{V}$ at each terminal, until they coincide with the transfer plane, with the points $\mathcal{Q}_{01}$ and $\mathcal{Q}_{02}$ situated on the opposite sides of the axis of rotation, which is the coinciding constraining lines, Eq. (9) indicates that under optimum condition, the two velocity-increment vectors $\Delta\mathbf{V}_1$ and $\Delta\mathbf{V}_2$ are collinear. The geometry is shown in the second simplified hodograph diagram in Fig. 3b. It is interesting to note that the present consideration has actually reduced the problem of two-impulse optimal transfer to the popular Spider-Fly problem[9] with the position-space replaced by the velocity-space. Now with reference to the second simplified hodograph diagram, the two-impulse optimal point Q_{**} can be readily determined by straight line construction once the two terminal velocity points $\mathcal{Q}_{01}$ and $\mathcal{Q}_{02}$ are located, and the analytic solution follows immediately by using elementary coordinate geometry. It is worth noting here that the minimum total velocity impulse f_{**} may be determined from such a simplified diagram without first determining the two terminal impulses, since it is simply the distance between the two points $\mathcal{Q}_{01}$ and $\mathcal{Q}_{02}$ in the diagram. The principal results are summarized below:

$$_{**} = \{[V_{0r1} + V_{0r2}]^2 + [(V_{0\Theta 1}{}^2 - 2A_1V_{0\Theta 1}\cos\omega_1 A_1{}^2)^{1/2} + (V_{0\Theta 2}{}^2 - 2A_2V_{0\Theta 2}\cos\omega_2 + A_2{}^2)^{1/2}]^2\}^{1/2} = \left(\frac{\mu}{r_1}\right)^{1/2}\left\{\left[\nu_{0r1} + \frac{1}{(n)^{1/2}}\nu_{0r2}\right]^2 + \left[\left(\nu_{0\Theta 1}{}^2 - 2\left\{\frac{2n}{n+1}\right\}^{1/2}\nu_{0\Theta 1}\cos\omega_1 + \frac{2n}{n+1}\right)^{1/2} + \frac{1}{(n)^{1/2}}\left(\nu_{0\Theta 2}{}^2 - 2\left\{\frac{2}{n+1}\right\}^{1/2}\nu_{0\Theta 2}\cos\omega_2 + \frac{2}{n+1}\right)^{1/2}\right]^2\right\}^{1/2} \tag{10}$$

$$\left(\frac{f}{f_1}\right)_{**} = 1 + \left(\frac{V_{0\Theta 2}{}^2 - 2A_2V_{0\Theta 2}\cos\omega_2 + A_2{}^2}{V_{0\Theta 1}{}^2 - 2A_1V_{0\Theta 1}\cos\omega_1 + A_1{}^2}\right)^{1/2} = 1 + \frac{1}{(n)^{1/2}}\left(\frac{\nu_{0\Theta 2}{}^2 - 2\left\{\frac{2}{n+1}\right\}^{1/2}\nu_{0\Theta 2}\cos\omega_2 + \frac{2}{n+1}}{\nu_{0\Theta 1}{}^2 - 2\left\{\frac{2n}{n+1}\right\}^{1/2}\nu_{0\Theta 1}\cos\omega_1 + \frac{2n}{n+1}}\right)^{1/2} \tag{11a}$$

$$\left(\frac{f}{f_2}\right)_{**} = 1 + \left(\frac{V_{0\Theta 1}{}^2 - 2A_1V_{0\Theta 1}\cos\omega_1 + A_1{}^2}{V_{0\Theta 2}{}^2 - 2A_2V_{0\Theta 2}\cos\omega_2 + A_2{}^2}\right)^{1/2} = 1 + (n)^{1/2}\left(\frac{\nu_{0\Theta 1}{}^2 - 2\left\{\frac{2n}{n+1}\right\}^{1/2}\nu_{0\Theta 1}\cos\omega_1 + \frac{2n}{n+1}}{\nu_{0\Theta 2}{}^2 - 2\left\{\frac{2}{n+1}\right\}^{1/2}\nu_{0\Theta 2}\cos\omega_2 + \frac{2}{n+1}}\right)^{1/2} \tag{11b}$$

$$\gamma_{\Delta 1} = \pi - \gamma_{\Delta 2} = \tan^{-1}\left[-\frac{(V_{0\Theta 1}{}^2 - 2A_1V_{0\Theta 1}\cos\omega_1 + A_1{}^2)^{1/2} + (V_{0\Theta 2}{}^2 - 2A_2V_{0\Theta 2}\cos\omega_2 + A_2{}^2)^{1/2}}{V_{0r1} + V_{0r2}}\right]$$

$$= \tan^{-1}\left[-\frac{\left(\nu_{0\Theta 1}{}^2 - 2\left\{\frac{2n}{n+1}\right\}^{1/2}\nu_{0\Theta 2}\cos\omega_1 + \frac{2n}{n+1}\right)^{1/2} + \frac{1}{(n)^{1/2}}\left(\nu_{0\Theta 2}{}^2 - 2\left\{\frac{2}{n+1}\right\}^{1/2}\nu_{0\Theta 2}\cos\omega_2 - \frac{2}{n+1}\right)^{1/2}}{\nu_{0r1} + \frac{1}{(n)^{1/2}}\nu_{0r2}}\right] \tag{12}$$

$$\Lambda_1 = \sin^{-1}\frac{V_{0\Theta 1}\sin\omega_1}{(V_{0\Theta 1}{}^2 - 2A_1V_{0\Theta 1}\cos\omega_1 + A_1{}^2)^{1/2}} = \sin^{-1}\frac{\nu_{0\Theta 1}\sin\omega_1}{\left(\nu_{0\Theta 1}{}^2 - 2\left\{\frac{2n}{n+1}\right\}^{1/2}\nu_{0\Theta 2}\cos\omega_1 + \frac{2n}{n+1}\right)^{1/2}} \tag{13a}$$

$$\Lambda_2 = \sin^{-1}\frac{-V_{0\Theta 2}\sin\omega_2}{(V_{0\Theta 2}{}^2 - 2A_2V_{0\Theta 2}\cos\omega_2 + A_2{}^2)^{1/2}} = \sin^{-1}\frac{-\nu_{0\Theta 2}\sin\omega_2}{\left(\nu_{0\Theta 2}{}^2 - 2\left\{\frac{2}{n+1}\right\}^{1/2}\nu_{0\Theta 2}\cos\omega_2 + \frac{2}{n+1}\right)^{1/2}} \tag{13b}$$

Note here the second form of each of the Eqs. (10–13) is in the nondimensional parameters ν_{0ri}, $\nu_{0\Theta i}$, ω_i ($i = 1,2$), and n. For symbols, see Nomenclature and Figs. 1–3.

III. Optimal Orientation of the Transfer Plane

The optimal total velocity impulse f_{**} in the preceding solution, Eq. (10), will now be further minimized with respect to the orientation of the transfer plane, defined by ω_1 and ω_2, for a fixed oblique angle σ between the two terminal orbit planes. The stationarity condition $df_{**} = 0$ under the constraint equation (3) yields the optimal orientation equation,

$$\frac{\sin\omega_{2**}}{\sin\omega_{1**}} = -n\left(\frac{1 - 2\rho_2\cos\omega_{2**} + \rho_2{}^2}{1 - 2\rho_1\cos\omega_{1**} + \rho_1{}^2}\right)^{1/2} \tag{14}$$

where

$$\rho_1 = A_1/V_{0\Theta 1}, \qquad \rho_2 = A_2/V_{0\Theta 2}, \qquad n = r_2/r_1 \tag{15}$$

The pair of equations (3) and (14) determines the optimal values ω_{1**} and ω_{2**}. Some typical optimal orientation curves defined by Eq. (14) are shown in Fig. 4. The intersection of the straight line σ = const with the optimal curve gives the optimal solution point for a given σ. The locus defined by Eq. (14) is symmetric with respect to the origin, and contains more than the solution points. Figure 4 shows only the branch of the locus in the 4th quadrant of the ω_1,ω_2 plane, pertaining to the absolute minimum f_{**} solution. It is evident that all solution points are confined in this quadrant, and we have

$$0 \leqslant \omega_{1**} \leqslant \sigma, \; -\sigma \leqslant \omega_{2**} \leqslant 0$$

The variation of the optimal angles ω_{1**} and $-\omega_{2**}$ with the distance ratio n and the oblique orbital angle σ are shown in Figs. 5 and 6.

A study of the optimal orientation locus in the ω_1,ω_2 plane shows that it is either of the type A, or of the type B, as indicated in Fig. 4. On the type A curve there is a maximum $|\omega_{2**}|$, and on the type B curve, a maximum ω_{1**}. Thus under constant values of $\nu_{0\Theta 1}$, $\nu_{0\Theta 2}$, and n, as σ varies from zero to 180°, the optimal inclination of the transfer plane with one of the terminal orbit plane is restricted, whereas that with the other may vary in the full range of zero to 180°. Under particular terminal conditions, the curve may become the J type, that is the joint type, which consists of a type A branch and a type B branch joined at the point J, as shown in Fig. 4. The type of the optimal orientation curve is determined by the values of $V_{0\Theta 1}$, $V_{0\Theta 2}$, and n, as depicted in the region diagram in the hodograph plane in Table 1. The coordinates of the points of maximum inclinations (magnitudes) are given in Table 2.

Before proceeding to further analysis it is well to note here that the optimal condition (14) implies

$$\sin\Lambda_2/\sin\Lambda_1 = n \tag{16}$$

which can be readily seen from the hodograph geometry (Fig. 2). Thus, for optimal transfer, the inclinations of the two velocity-increment planes with the transfer plane satisfy Snell's Law of Refraction, with the distance ratio n as the index of refraction.

IV. Coplanar Case

The preceding analytic solution holds for the noncoplanar transfer as well as the coplanar transfer. In the latter case, the transfer plane is of course the common orbital plane; however, there are two subcases to be distinguished: 1) the

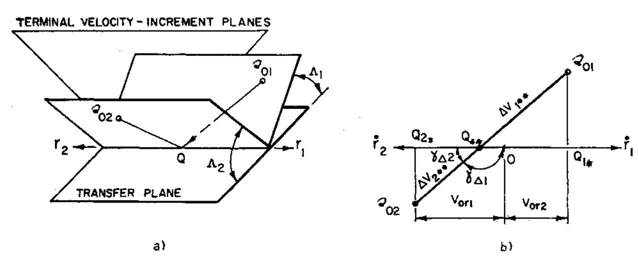

Fig. 3 The simplified hodograph diagrams for the optimal 2-impulse 180° transfer.

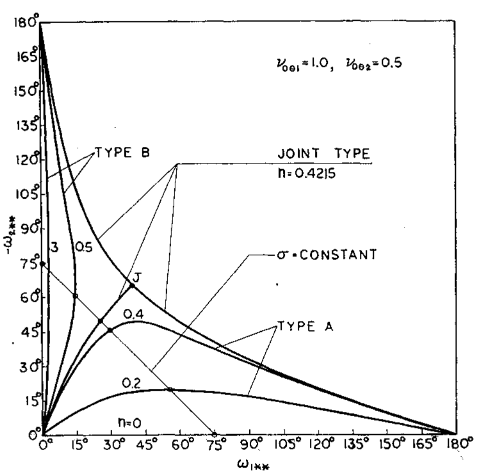

Fig. 4 Typical orientation curves for the optimal transfer plane.

Table 1 Hodograph regions and the types of the optimal orientation curves

	REGION DIAGRAM	BOUNDARY RELATIONS	
n<1	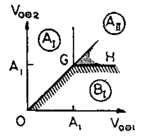	OG $\nu_{o\theta 2}^2 = n\nu_{o\theta 1}^2$, $\nu_{o\theta 1}^2 \leq \frac{2n}{n+1}$	(A-1)
		GH $\nu_{o\theta 2}^2 = \frac{2n^2}{n+1}$, $\nu_{o\theta 1}^2 \geq \frac{2n}{n+1}$	(A-2)
n>1	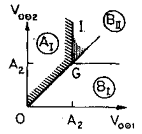	OG $\nu_{o\theta 2}^2 = n\nu_{o\theta 1}^2$, $\nu_{o\theta 1}^2 \leq \frac{2}{n(n+1)}$	(A-3)
		GI $\nu_{o\theta 1}^2 = \frac{2}{n(n+1)}$, $\nu_{o\theta 2}^2 \geq \frac{2}{n+1}$	(A-4)
n=1	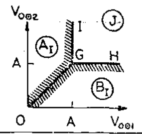	OG $\nu_{o\theta 1} = \nu_{o\theta 2} \leq 1$	(A-5)
		GHI (region) $\nu_{o\theta 1} \geq 1$, $\nu_{o\theta 2} \geq 1$	(A-6)

Regions: A_I, A_{II}, optimal curve type A; B_I, B_{II}, optimal curve type B; on boundary and in region J, optimal curve type J.
Shaded area, limited inclination with the orbit plane at slower terminal.

two terminal orbits are of the same rotational sense, and 2) they are of opposite senses. The former is characterized by $\sigma = 0$, the latter by $\sigma = \pi$.

In case 1, evidently we have $\omega_{1**} = 0$, $\omega_{2**} = 0$; the transfer trajectory is of the same sense as that of the terminal orbits. The solution is unique. In case 2, a study of the hodograph geometry shows that there are two local minimal solutions, one in each sense. Solution I is given by $\omega_{1**} = 0$, where the transfer is in the sense of the initial orbit; whereas in solution II, given by $\omega_{2**} = 0$, the transfer is in the sense of the final orbit. If no particular sense of motion is preferred, then an absolute minimal solution may be chosen. It is clear from the previous study of the optimal orientation curves that solution I gives the absolute minimum f_{**} if the curve is of type B, and that solution II will be so if it is of type A. In case the curve is of the J type, then the two minimal solutions give the same f_{**}, and we have a double minimum. The analytic solutions for the coplanar case are summarized in Table 3, which contain the Hohmann solution as a particular case ($\sigma = 0$, $\nu_{0r1} = \nu_{0r2} = 0$, $\nu_{0\theta 1} = \nu_{0\theta 2} = 1$).

V. Multiminimum Solution

The analytic solution for the optimal transfer in an arbitrary transfer plane is unique. However, as seen in the preceding section, a double minimum may arise in the case of the transfer between two coplanar orbits of opposite senses. Such a situation may also arise in the noncoplanar case when the transfer plane is open to choice. A study of the optimal orientation locus, defined by Eq. (14) and graphically depicted in Fig. 4, shows that the constant-σ line may cut the optimal curve in two distinct points when the latter is of the joint type. In such a case there are two distinct transfer planes for choice: one closer to the initial orbit plane, and

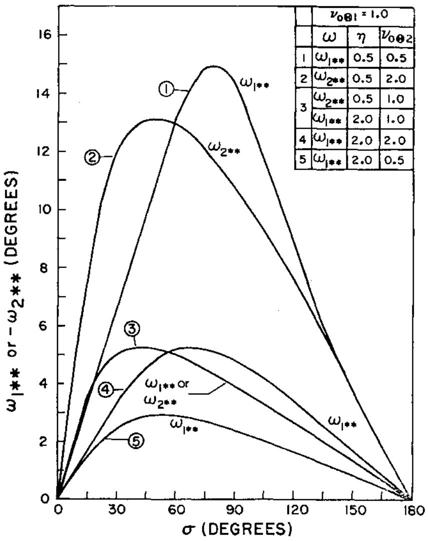

Fig. 5 The optimal inclination of the transfer plane vs the angle between terminal orbit planes.

the other closer to the final orbit plane; both yield the same f_{**}, a double minimum. As established in Ref. 12, no multiplicity higher than two may arise in the 180° transfer.

VI. Effects of Terminal Conditions on the Optimal Solution

A. Primary Observations

Based on the analytic solution in Section II and the optimal orientation equation (14), two primary observations may now be made: 1) The radial components of the terminal velocities have no effects on the optimal orientation of the transfer plane, and they affect the total minimum velocity impulse and the terminal velocity impulses only through their algebraic sum, but not individually; and 2) for a fixed oblique orbital angle σ, the optimal orientation of the transfer plane is determined by the three ratios: ρ_1, ρ_2, and n, defined by Eqs. (15), or, equivalently, the three parameters: $\nu_{0\theta 1}$, $\nu_{0\theta 2}$, and n.

B. Optimal Transfer Plane

An important feature of the optimal transfer plane, as shown in Sec. III, is that, under fixed terminal conditions defined by $\nu_{0\theta 1}$, $\nu_{0\theta 2}$, and n, its inclination with one of the terminal orbit planes is usually highly limited (optimal orientation curve of type A or B). When this is the case, the orientation of the optimal transfer plane will never deviate too far from that of one of the terminal orbit planes, whereas the oblique orbital angle σ may vary from zero to 180°. The corresponding terminal plane in such a case will be referred to as the major orbit plane. A study of the region diagram in Table 1

Table 2 Coordinates of the points of maximum inclination of the optimal transfer plane

Hodograph region	Coordinates	
$A_{\rm I}$	$\cos\omega_{1**} = \dfrac{1}{\rho_1}$, $\cos\lvert\omega_{2**}\rvert_{\max} = \dfrac{n^2\rho_2}{\rho_1^2} + \left[\left(1 - \dfrac{n^2}{\rho_1^2}\right)\left(1 - \dfrac{n^2\rho_2^2}{\rho_1^2}\right)\right]^{1/2}$	(B-1)
$A_{\rm II}$ ($n < 1$)	$\cos\omega_{1**} = \rho_1$, $\cos\lvert\omega_{2**}\rvert_{\max} = n^2\rho_2 + [(1 - n^2)(1 - n^2\rho_2^2)]^{1/2}$	(B-2)
$B_{\rm II}$ ($n > 1$)	$\cos(\omega_{1**})_{\max} = \dfrac{\rho_1}{n^2} + \left[\left(1 - \dfrac{1}{n^2}\right)\left(1 - \dfrac{\rho_1^2}{n^2}\right)\right]^{1/2}$, $\cos\omega_{2**} = \rho_2$	(B-3)
$B_{\rm I}$	$\cos(\omega_{1**})_{\max} = \dfrac{\rho_1}{n^2\rho_2^2} + \left[\left(1 - \dfrac{1}{n^2\rho_2^2}\right)\left(1 - \dfrac{\rho_1^2}{n^2\rho_2^2}\right)\right]^{1/2}$, $\cos\omega_2{}^{**} = \dfrac{1}{\rho_2}$	(B-4)

Table 3 Minimum impulse solution for two-impulse 180° transfer between Keplerian orbits: coplanar case[a]

	Symbol	Terminal orbits of the same sense ($\sigma = 0$)	
Total velocity impulse, nondimensional	$\frac{f_{**}}{(\mu/r_1)^{1/2}}$	$\left[\left(\nu_{0r1} + \frac{1}{\{n\}^{1/2}}\nu_{0r2}\right)^2 + \left(\left\|\nu_{0\Theta1} - \left\{\frac{2n}{n+1}\right\}^{1/2}\right\| + \frac{1}{\{n\}^{1/2}}\left\|\nu_{0\Theta2} - \left\{\frac{2}{n+1}\right\}^{1/2}\right\|\right)^2\right]^{1/2}$	(C-1a)
Initial-to-total velocity impulse	$\left(\frac{f_1}{f}\right)_{**}$	$\left[1 + \left\|\frac{\nu_{0\Theta2} - \left(\frac{2}{n+1}\right)^{1/2}}{(n)^{1/2}\left(\nu_{0\Theta1} - \left\{\frac{2n}{n+1}\right\}^{1/2}\right)}\right\|\right]^{-1}$	(C-2a)
Final-to-total velocity impulse	$\left(\frac{f_2}{f}\right)_{**}$	$\left[1 + \left\|\frac{(n)^{1/2}\left(\nu_{0\Theta1} - \left\{\frac{2n}{n+1}\right\}^{1/2}\right)}{\nu_{0\Theta2} - \left(\frac{2}{n+1}\right)^{1/2}}\right\|\right]^{-1}$	(C-3a)
Direction angles of terminal increments	$(\gamma_{\Delta1})_{**} = \pi - (\gamma_{\Delta2})_{**}$	$\tan^{-1}\left[-\frac{\left\|\nu_{0\Theta1} - \left(\frac{2n}{n+1}\right)^{1/2}\right\| + \frac{1}{(n)^{1/2}}\left\|\nu_{0\Theta2} - \left(\frac{2}{n+1}\right)^{1/2}\right\|}{\nu_{0r1} + \frac{1}{(n)^{1/2}}\nu_{0r2}}\right]$	(C-4a)
	Symbol	Terminal orbits of opposite senses ($\sigma = \pi$)	
Total velocity impulse, nondimensional	$\frac{f_{**}}{(\mu/r_1)^{1/2}}$	$\left[\left(\nu_{0r1} + \frac{1}{\{n\}^{1/2}}\nu_{0r2}\right)^2 + \left(\left\|\nu_{0\Theta1} \mp \left\{\frac{2n}{n+1}\right\}^{1/2}\right\| + \frac{1}{\{n\}^{1/2}}\left\|\nu_{0\Theta2} \pm \left\{\frac{2}{n+1}\right\}^{1/2}\right\|\right)^2\right]^{1/2}$	(C-1b)
Initial-to-total velocity impulse	$\left(\frac{f_1}{f}\right)_{**}$	$\left[1 + \left\|\frac{\nu_{0\Theta2} \pm \left(\frac{2}{n+1}\right)^{1/2}}{(n)^{1/2}\left(\nu_{0\Theta1} \mp \left\{\frac{2n}{n+1}\right\}^{1/2}\right)}\right\|\right]^{-1}$	(C-2b)
Final-to-total velocity impulse	$\left(\frac{f_2}{f}\right)_{**}$	$\left[1 + \left\|\frac{(n)^{1/2}\left(\nu_{0\Theta1} \mp \left\{\frac{2n}{n+1}\right\}^{1/2}\right)}{\nu_{0\Theta2} \pm \left(\frac{2}{n+1}\right)^{1/2}}\right\|\right]^{-1}$	(C-3b)
Direction angles of terminal increments	$(\gamma_{\Delta1})_{**} = \pi - (\gamma_{\Delta2})_{**}$	$\tan^{-1}\left[-\frac{\left\|\nu_{0\Theta1} \mp \left(\frac{2n}{n+1}\right)^{1/2}\right\| + \frac{1}{(n)^{1/2}}\left\|\nu_{0\Theta2} \pm \left(\frac{2}{n+1}\right)^{1/2}\right\|}{\nu_{0r1} + \frac{1}{(n)^{1/2}}\nu_{0r2}}\right]$	(C-4b)

[a] Two solutions: upper signs for the transfer in the sense of the initial orbit; lower signs, in the sense of the final orbit.

shows that the major orbit plane will be either at the terminal closer to the field center (nearer terminal), or at the terminal with higher transversal velocity component (fast terminal). In the special case, wherein the terminal parameters $\nu_{0\Theta1}$, $\nu_{0\Theta2}$, and n satisfy the boundary relations in Table 1, the optimal orientation curve is of the joint type, and the distinction between major and minor orbit planes ceases to make sense. Criteria concerning the major orbit planes are summarized in Table 4.

Table 4 Terminal conditions and the major orbit plane

Terminal conditions[a]		Major orbit plane
$r_1 \neq r_2$, $V_{0\Theta1} \neq V_{0\Theta2}$	1) $V_{0\Theta k} > A_j$	At nearer terminal, regardless of $V_{0\Theta2}/V_{0\Theta1}$.
	2) $V_{0\Theta k} < A_j$	At faster terminal, regardless of n.
	3) $V_{0\Theta k} = A_j$	No distinction.
$r_1 \neq r_2$, $V_{0\Theta1} = V_{0\Theta2}$ ($\equiv V_{0\Theta}$)	1) $V_{0\Theta} > A_j$	At nearer terminal.
	2) $V_{0\Theta} \leq A$	No distinction.
$r_1 = r_2$, $V_{0\Theta1} \neq V_{0\Theta2}$ ($A_1 = A_2 \equiv A$)	1) $V_{0\Theta1} \leq A$ and/or $V_{0\Theta2} \leq A$	At faster terminal.
	2) $V_{0\Theta1} \geq A$, $V_{0\Theta2} \geq A$	No distinction.
$r_1 = r_2$, $V_{0\Theta1} = V_{0\Theta2}$		No distinction.

[a] $V_{0\Theta k}$ = smaller one of $V_{0\Theta1}$ and $V_{0\Theta2}$; A_j = smaller one of A_1 and A_2.

When the terminal velocity parameters $\nu_{0\Theta1}$ and $\nu_{0\Theta2}$ are fixed while n varies, the major plane will be at the final terminal for values of $n < n_J$, and at the initial terminal for $n > n_J$, where n_J is the value of n on the boundary in the region diagram (Table 1). The shift of the major plane from one terminal to the other occurs at $n = n_J$.

Under constant terminal distances and transversal velocities, the optimal transfer plane is close to the major orbit plane at low values of σ close to zero and also at high values of σ close to 180°, and its maximum directional deviation from the major plane usually occurs in the intermediate range of σ. At low σ, the numerical difference between ω_{1**} and ω_{2**} is small, of course. However, at large values of σ the optimal transfer plane will be far closer to the major plane than to the other, if n is not close to n_J.

As an illustration, we note from Figs. 5 and 6b that under the terminal condition $\nu_{0\Theta1} = \nu_{0\Theta2} = 1$ the maximum deviation of the optimal transfer plane from the major plane, the initial plane in this case, is about 5.25° when $n = \frac{1}{2}$, which occurs at $\sigma = 45°$, and the maximum deviation from the major plane does not exceed 5.265° for all values of n (0 to ∞), and σ (0–180°). This case is worth notice as it embraces the popular case of circle-to-circle transfer. The deviation is exceedingly small in this particular case. However, it may become considerably large under other terminal conditions. For example, in the case of $\nu_{0\Theta1} = 1$, $\nu_{0\Theta2} = 0.5$, and $n = 0.4$, we

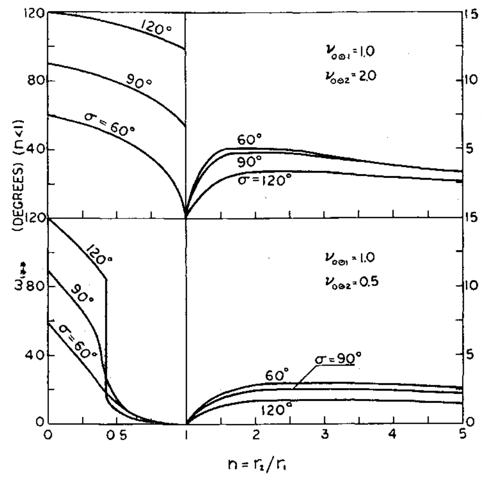

Fig. 6a The optimal inclination of the transfer plane vs distance ratio ($v_o\theta_1 = 1$, $v_o\theta_2 = 0.5, 2.0$).

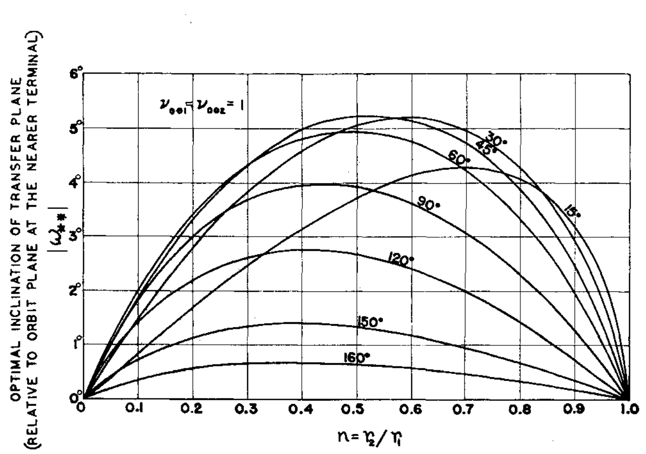

Fig. 6b The optimal inclination of the transfer plane vs distance ratio ($v_o\theta_1 = v_o\theta_2 = 1$).

found that the maximum deviation from the major plane is about 47°, which occurs at $\sigma \cong 90°$ (see Fig. 4).

C. Minimum Total Impulse

For comparison purpose, the minimum total velocity impulses required for the transfer under several typical terminal conditions were calculated from the analytic solution for the three modes of transfer: the transfer in the initial orbit plane ($\omega_1 = 0$), in the final orbit plane ($\omega_2 = 0$), and in the optimal plane. The results are shown graphically in Figs. 7 and 8. These calculations were based on the assumption of zero radial components of the terminal velocities. However, the following observations made on these results hold as well for the case in which these components are nonzero, since the presence of the radial components do not alter the optimal transfer plane:

1) For a given angle between the terminal orbit planes, the higher the distance ratio, the smaller the total impulse ratio $f_{**}/(\mu/r_1)^{1/2}$ required for all three modes of transfer. Thus with a given departure terminal, the farther the target terminal, the more economic is the transfer.

2) When the distance ratio increases under constant terminal velocity parameters ν_{01} and ν_{02}, the optimal plane solution first follows closely the final plane solution ($\omega_2 = 0$) at low values of n, and then follows closely the initial plane solution ($\omega_1 = 0$) at high values of n. The saving in the total velocity impulse by optimizing the transfer plane is seen to be very small in the extreme ranges of values of n, very small and very large. It becomes appreciable only in the inter-

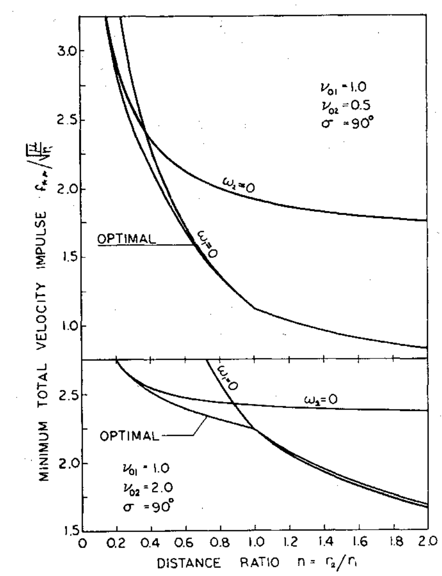

Fig. 7 The minimum total velocity impulse vs distance ratio under different modes of transfer.

mediate range of n. This is true for all values of σ. Figure 7 shows that in the case of $\nu_{01} = 1$, $\nu_{02} = 2$, and $\sigma = 90°$ this ranges from about $n = 0.2$ to 1.0, with a maximum saving of 5.8% at $n = 0.88$ where the initial plane solution and the final plane solution are equal.

3) At constant terminal distances and terminal velocities, the minimum total velocity impulse increases with the oblique orbital angle σ for all three modes of transfer.

4) Under the same conditions mentioned previously, the optimal solution follows either the initial plane solution or the final plane solution, depending on which is the major one, throughout the whole range of $\sigma = 0$ to 180° (σ does not affect the location of the major plane!). The saving in minimum total velocity impulse by using the optimal transfer plane is small at small σ (close to 0), and at large σ (close to 180°), with significant saving occurring in some intermediate range of σ. In the case illustrated in Fig. 8, in which ν_{01} =

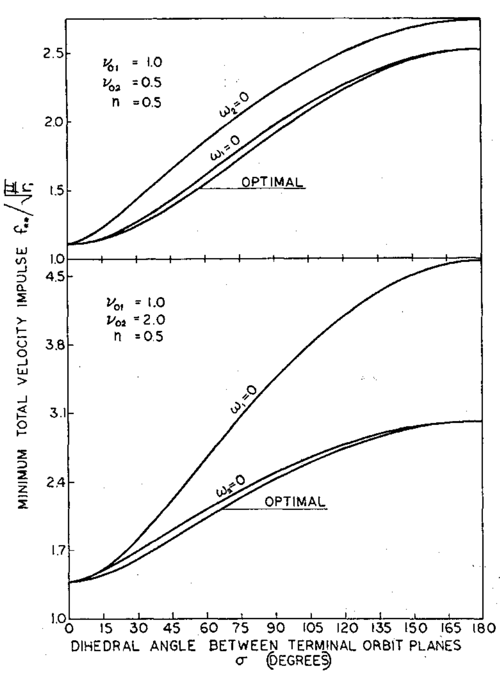

Fig. 8 The minimum total velocity impulse vs the angle between terminal orbit planes under different modes of transfer.

1, $\nu_{02} = 2$, and $n = \frac{1}{2}$, this range is approximately $\sigma = 5°$ to 150°, with a maximum saving of 5% at $\sigma \cong 36°$.

5) Under fixed terminal velocity parameters ν_{01} and ν_{02} the difference between the initial plane solution and the final plane solution increases monotonically with σ throughout the range, 0–180°, at constant n, and this difference may become quite large as σ increases. At constant σ, this difference is large at extreme values of n, very large or very small (see Fig. 7).

VII. Concluding Remarks

In the light of the foregoing observations, the directional deviation of the optimal transfer plane from the major terminal plane is generally small in the extreme ranges of n (very high and very low) and σ (close to 0 or 180°). Thus, we may say that in general the optimal orientation of the transfer plane favors that of the major terminal plane in these extreme ranges of terminal conditions, and the corresponding saving in the total velocity impulse from optimizing the orientation of the transfer plane is small. This justifies the planar treatment of many cases that are actually noncoplanar and, in particular, the case of transfers under circular or near-circular transversal terminal velocities ($\nu_{0\Theta 1} \cong 1$, $\nu_{0\Theta 2} \cong 1$), in which the optimal transfer plane is seen to be close to the major terminal plane throughout the whole range of terminal conditions ($n = 0$–∞, $\sigma = 0$–180°). However, when the terminal transversal velocities are noncircular, the saving in the total velocity impulse is appreciable in the intermediate ranges of n and σ, and the optimization of the transfer plane is of significance.

Although the difference between the optimal plane solution and the major terminal plane solution is usually small, the difference between the initial plane solution and the final plane solution may be very large. This is especially so when the oblique orbital angle is large, and the distance ratio is very low or very high. Thus, if no optimization of the transfer plane is attempted, the choice of the transfer plane from the two terminal orbit planes is of paramount importance. In this connection the criteria provided in the preceding section concerning the major terminal planes should be helpful.

In orbital transfer problems in which the change of orbital plane is necessary, it is a general belief that the change should be made at the slower terminal, that is, where the terminal orbit velocity is smaller. This implies that the optimal orientation of the transfer plane generally favors that of the orbit plane at the faster terminal. However, the present analysis shows that this is not necessarily true in a 180° transfer. First, it is the transversal components of the terminal velocities that determine the major terminal plane, not the total terminal velocities. Hence, in this connection, the term faster or slower should refer to these components only, not to the total terminal velocities. Second, the major orbit plane, though it is located at the faster terminal in most cases, there are velocity regions in which the orbit plane at the slower terminal is the major one (see hatched area in Table 1). Hence it is quite possible that the change of orbital plane is to be made at the faster terminal.

In the planar treatment of the transfer problems, it is generally assumed that the oblique orbital angle is either zero or very small. The present analysis shows that such a treatment should also be applicable to the cases where σ is close to 180°, since the directional deviation of the optimal transfer plane from the major terminal orbit plane is also small at high oblique orbital angle. Here again the determination of the major orbit plane is important.

In all the foregoing analyses and discussions, it has been tacitly assumed that the optimal solution is realistic, that is, the optimal transfer trajectory contains no points at infinity. However, as shown in Ref. 12, an unrealistic optimum may arise in the two-impulse transfer through any arbitrary range angle including 180°. In this connection, the following criteria for the 180° case is useful:

$$
\begin{aligned}
|V_r| &< \left(\frac{2\mu}{r_1 + r_2}\right)^{1/2} \text{ realistic, elliptic} \\
V_r &= -\left(\frac{2\mu}{r_1 + r_2}\right)^{1/2} \text{ realistic, parabolic} \\
V_r &< -\left(\frac{2\mu}{r_1 + r_2}\right)^{1/2} \text{ realistic, hyperbolic} \\
V_r &\geqq +\left(\frac{2\mu}{r_1 + r_2}\right)^{1/2} \text{ unrealistic}
\end{aligned}
\tag{17}
$$

where V_r is the radial component of the transfer velocity at either terminal point, taken positive in the direction of $\mathbf{r}_1$, and, in the transfer in the optimal plane, it is given by

$$
V_{r**} = \frac{r_1 V_{0r1} \csc\omega_{1**} + r_2 V_{0r2} \csc\omega_{2**}}{r_1 \csc\omega_{1**} - r_2 \csc\omega_{2**}} \tag{18}
$$

Thus the radial components of the terminal velocities, though they have no effect on the optimal orientation of the transfer plane when the optimal solution is realistic, play an important role in determining the type and hence the nature of the optimal transfer trajectory. Whenever an unrealistic optimum arises, the realistic solution becomes indefinite, and the radial components will further affect the optimal orientation of the transfer plane, depending on the realistic optimum trajectory chosen.

Finally, it is to be noted that the present solution is optimal under the assumption of fixed number of impulses, $N = 2$, and fixed range angle, $\psi = 180°$. No absolute optimality is assured when N and/or ψ are open to choice. Current research[2,10,11] indicates that the two-impulse, 180° solution is indeed the global optimum in some cases, and there are also other cases, where three or more impulses are more economical than two impulses. Such extensive discussions, however, are beyond the scope of the present paper.

References

[1] Hohmann, W., *Die Errichbarkeit der Himmelskörper*, Oldenbourg, Munich, 1925.

[2] Hoelker, R. F. and Silber, R., "The Bielliptical Transfer Between Coplanar Circular Orbits," *Ballistic Missiles and Space Technology*, Vol. III, Pergamon, New York, 1961, pp. 164–175.

[3] Lawden, D. F., "Impulsive Transfer Between Elliptical Orbits," *Optimization Techniques*, edited by G. Leitmann, Academic Press, New York, 1962, pp. 333–348.

[4] Sun, F. T., "On the Hodograph Method for Solution of Orbit Problems," *Proceedings of the 12th International Astronautical Congress*, Vol. II, 1963, pp. 879–915.

[5] Ehricke, K. A., *Space Flight*, Vol. II, Van Nostrand, Princeton, N. J., 1962, pp. 383–385.

[6] Altman, S. P. and Pistiner, J. S., "Analysis of the Orbital Transfer Problem in Three-Dimensional Space," *AIAA Progress in Astronautics and Aeronautics: Celestial Mechanics and Astrodynamics*, Vol. 14, edited by V. G. Szebehely, Academic Press, New York, 1964, pp. 627–654.

[7] Lee, G., "An Analysis of Two-Impulse Orbital Transfer," *AIAA Journal*, Vol. 2, No. 10, Oct. 1964, pp. 1767–1773.

[8] Sun, F. T., "Hodograph Analysis of the Free-Flight Trajectories Between Two Arbitrary Terminal Points," CR-153, Jan. 1965, NASA.

[9] Tietze, H., *Famous Problems of Mathematics*, Graylock Press, New York, 1965, pp. 38, 44–45.

[10] Edelbaum, T. N., "Minimum Impulse Transfers in the Near Vicinity of a Circular Orbit," *Journal of the Astronautical Sciences*, Vol. XIV, No. 2, March–April 1967, pp. 66–73.

[11] Marchal, C., Marec, J. P., and Winn, C. B., "Synthese des resultats analytiques sur les transferts optimaux entre orbits Kepleriennes," 18th IAF Congress, Belgrade, 1967, International Astronautical Federation; also TT F-11, 590, 1968, NASA.

[12] Sun, F. T., "Analysis of the Optimum Two-Impulse Orbital Transfer under Arbitrary Terminal Conditions," *AIAA Journal*, Vol. 6, No. 11, Nov. 1968, pp. 2145–2153.